PHYSICAL REVIEW B VOLUME 27, NUMBER 2 15 JANUARY 1983

Vibrational properties of crystalline group-VI solids: Te, Se, S

P. J. Carroll
Bell Telephone Laboratories, Murray Hill, New Jersey 07974*
and Department of Physics, The Pennsylvania State University, University Park, Pennsylvania 16802

J. S. Lannin
Department of Physics, The Pennsylvania State University, University Park, Pennsylvania 16802
(Received 13 August 1982)

Second-order Raman scattering is reported in the elemental crystalline group-VI systems of trigonal Te and Se, composed of chains, as well as monoclinic Se-ring and orthorhombic S-ring systems. As in elemental semiconductors and semimetals, the spectra are interpreted in terms of predominant overtone scattering that manifests features in the one-phonon density of states. For the chain structures the phonon spectra yield reasonable agreement with previous valence force models, although differences exist at high frequencies near the maximum phonon range. A comparison of the second-order spectra for the highest optic band indicates trends in the phonon spectra in the sequence *t*-Te, *t*-Se, *m*-Se, and *o*-S that are indicative of increasing molecular character associated with reduced interunit interactions. In contrast to chain structures, the ring systems are shown to indicate additional features in the phonon density of states. This is also observed in the corresponding noncrystalline phases.

I. INTRODUCTION

In the elemental group-VI series of Te, Se, and S, interesting trends are observed in bonding and physical properties that indicate a varying role of interactions within and between structural units. These units correspond in the crystalline phases to ordered chains or rings, the former present in trigonal (*t*-) Te and Se and the latter in monoclinic (*m*-) Se and orthorhombic (*o*-) S. While the chain systems have been relatively well studied by a variety of physical methods, including inelastic neutron scattering measurements,[1] more limited measurements have been performed in ring forms. The latter are known from their physical properties and crystal structures to be more molecular in character. This is, for example, observed in the optical spectra,[2] which indicate an increased energy gap. The transition from molecular to nonmolecular character is also noted, for example, in comparisons of the $k=0$ vibrational states of *t*-Se and *m*-Se.[3,4] A number of theoretical studies of *t*-Te and *t*-Se have considered a range of lattice-dynamics models in attempting to explain neutron scattering dispersion curves[5–7] as well as to understand the role of interactions within and between chains. In *t*-Te such interactions have developed metalliclike bonding character. In the opposite extreme *o*-S has been considered to have primary van der Waals coupling between S_8 molecules.

In this study second-order Raman scattering is employed to obtain information about the phonon density of states and bonding of crystalline group-VI materials. Such higher-order scattering has been shown to be a useful tool for obtaining the approximate form of the phonon spectrum in group-IV (Refs. 8 and 9) and groups-V (Refs. 10 and 11) semiconductors and semimetals in elemental and alloy form. A recent study in crystalline iodine, which has significant molecular character, has also suggested similar information.[12] The criterion for obtaining the general form of the phonon density of states from a second-order scattering probe is that overtone processes predominate over combination contributions. In addition, it is required that coupling parameters are a smooth function of frequency within a given spectral band. Currently, direct neutron scattering measurements of the form of the phonon density of states are rather limited in resolution for high-frequency phonons. As such, information about the form of the phonon density of states for such bands from overtone Raman scattering provides additional constraints upon lattice-dynamical models. The present study yields trends in the second-order vibrational spectra that are an indication of variations in phonon dispersion with changes in bonding character. In particular, the results directly indicate changes in the phonon density of states that are a manifestation of increased delocalized bonding in the transition from insulating *o*-S to narrow gap *t*-Te in which metalliclike interactions play a significant role.

Information about the form of the phonon density of states in group-VI chain and ring crystalline structures is also of interest in understanding the structure and vibrational properties of the corresponding amorphous and liquid forms. Previous comparisons[13] of the first-order Raman spectra of amorphous Te, Se, and S have been primarily based on information on the $k=0$ states of the crystalline phases. As the Raman spectra of noncrystalline solids is related to the one-phonon density of states, rather than selected $k=0$ modes, a more valid comparison of changes in the vibrational spectra thus requires more detailed crystalline density-of-states information, which may be available from second-order Raman scattering under the conditions indicated above.

II. EXPERIMENT

Backscattering Raman measurements were performed at 300 K with the incident field in the scattering plane. This corresponds to $H'H$ and VH scattering components, where H' refers to the refracted angle of $\sim 15°$. The spectrometer used was a Spex 1401 double monochromator with a Tandem 1442 third monochromator. The spectrometer was either scanned at a constant rate or stepped at discrete frequency intervals under the control of an Apple II microcomputer.

Raman scattering measurements were performed on a single crystal of t-Te, obtained from Professor K. Vedam of The Pennsylvania State University. The (0001) face was polished with Al_2O_3 and syton to minimize extraneous scattered light. The Ar-laser 5145-Å line with ~ 300 mW of power was used to obtain the second-order Raman spectra, with the sample placed in an argon atmosphere to avoid the possibility of oxide formation. Technical-grade polycrystalline o-S obtained from the Fisher Chemical Company was employed in this study. The face of the sample was polished by a similar method as t-Te. The 6764-Å Kr line was employed with ~ 48 mW of power as o-S is virtually transparent to this line. The Raman spectra of all selenium samples were taken using the 7525-Å Kr-laser line. Though in most cases selenium is not totally transparent to this radiation, the penetration depth is large, ~ 1 mm for a-Se and t-Se at 300 K. The use of semitransparent radiation minimizes the possibility of heating and photostructural effects in m-Se. Both powdered and single-crystal m-Se (α) were obtained from Dr. R. Zallen of Xerox Corporation. The powdered sample was placed into a glass capillary tube and measured using ~ 50 mW of power. The spectrum showed that a certain percentage of the sample had become t-Se at some time. A subtraction of the t-Se spectrum revealed the second-order Raman spectrum of m-Se. The spectrum reported here was obtained from an unoriented single crystal using ~ 7 mW of power, and was similar to that obtained on the powdered mixture, suggesting that orientational differences are not significant for m-Se.

III. RESULTS AND DISCUSSION

A. Second-order Raman spectra of t-Te and t-Se

Figure 1 indicates the two components of the second-order Raman spectra (SORS) obtained from the (0001) face of single-crystal Te. The spectra appear very similar. The $H'H$ and VH spectra vary as a^2+c^2 and c^2, respectively, where a and c are the components of the A and E Raman tensors, respectively. The difference spectra $H'H-VH$ thus yields information about the a component only. This difference spectrum is also very similar to that of the components shown.

For purposes of discussion, the spectra can be divided into three regions or bands, separated by relative minima at 207 and 243 cm^{-1}. The first band appears as a shoulder at 180 cm^{-1} on the tail of an intense first-order peak located at 142 cm^{-1}. A comparison with an approximate phonon density of states obtained by neutron scattering, (ρ_N) of Kotov *et al.*[14] shown in Fig. 2(b), indicates that this band lies in the region of overtone scattering from the lower optic-phonon branches $OP^{(1)}$. Similarly, the

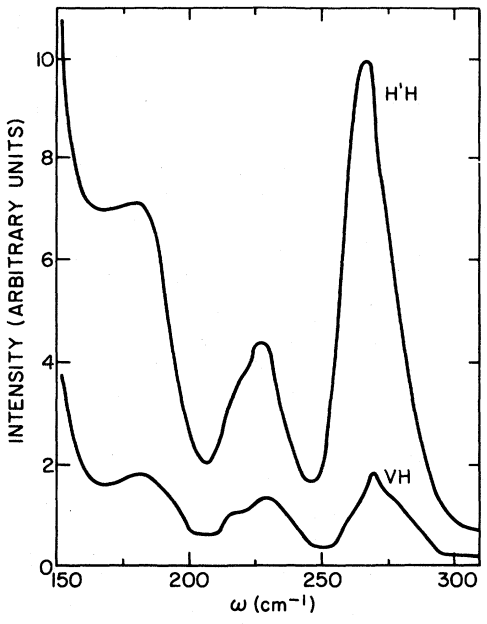

FIG. 1. Second-order Raman spectra of t-Te at 300 K.

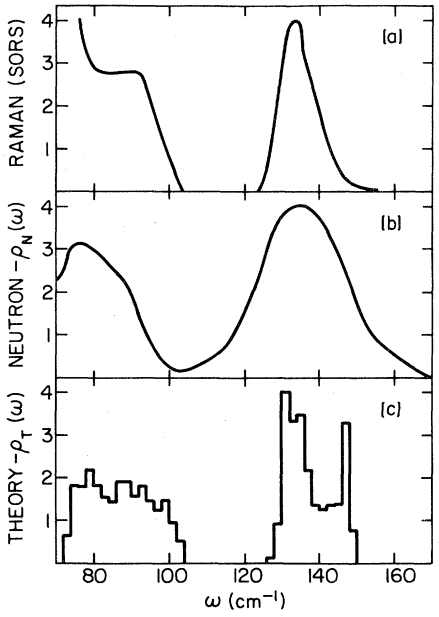

FIG. 2. Comparison of (a) the second-order Raman spectra of t-Te with (b) the neutron scattering—determined density of states of Ref. 14 and (c) the theoretical density of states of Ref. 18. The frequency scale in (a) has been halved for comparison.

band beyond 248 cm^{-1}, centered at 268 cm^{-1}, can be attributed to overtone scattering from the higher optic-phonon branches OP$^{(2)}$. The spectral band between 207 and 248 cm^{-1} lies in a region where all theoretical models[15–18] predict, and ρ_N shows, a gap in the density of states. This implies that this band originates from combination processes between the higher and lower optic-phonon branches. The peak of this band at 228 cm^{-1} is very near to half the value of the sum of the main peaks of the OP$^{(1)}$ and OP$^{(2)}$ bands. This is indirect evidence that the highest and lowest bands are primarily due to overtone processes. The relative intensity of the OP$^{(1)}$ and OP$^{(2)}$ combination band in Te is somewhat larger than that observed in the Raman spectra of other elemental semiconductors or semimetals.[5–12]

A variety of models have been used to obtain the phonon density of states of t-Te. Etchepare *et al.*[18] used perhaps the most detailed model. Their recent nine-parameter modified valence force-field fitted to neutron dispersion curves along high-symmetry directions yields the best agreement with experiment. Each of these models indicates reasonably good agreement with the SORS bands of t-Te which have been intepreted as overtones. In particular, a smoothing of each theoretical phonon density-of-states spectrum produces a shoulder at $\sim$90 cm^{-1} and a high-frequency band centered at $\sim$135 cm^{-1}, with a gap extending from $\sim$100 to $\sim$120 cm^{-1}. A number of models indicate, however, a large density of states in the OP$^{(2)}$ band to the low-frequency side of the peak at 135 cm^{-1} with a rapid decrease in the density of states thereafter. This does not agree with the SORS, which shows the OP$^{(2)}$ band rapidly rising to the peak at 2×134 cm^{-1} on the low-frequency side and exhibiting a shoulder on the high-frequency side.

In Fig. 2 the theoretical results of Etchepare *et al.* for the phonon density of states ρ_T is compared to neutron scattering results ρ_N and the SORS. The latter frequency scale has been halved for comparison. In obtaining Fig. 2(a) the combination band of Fig. 1 has been approximately subtracted by extrapolating the edges of the OP$^{(1)}$ and OP$^{(2)}$ associated bands. A smoothing of the histogram of $\rho_T(\omega)$ would produce a shoulder near 90 cm^{-1} and a band edge at 104 cm^{-1}, both of which agree with the Raman results. In addition, a smoothed histogram would also show a peak in the OP$^{(1)}$ band at 78 cm^{-1}. While this is in good agreement with a peak in $\rho_N(\omega)$, unfortunately the SORS is obscured by the tail of the intense first-order peak.

The maximum intensity of the OP$^{(2)}$ band in the SORS occurs at 2×134 cm^{-1}. This is in good agreement with both ρ_N and ρ_T. The shape of the band, which includes a shoulder at $\sim2\times139$ cm^{-1}, cannot be seen in ρ_N due to limited resolution. The effect of this limited resolution is evident in the ρ_N spectrum by the broadness of the high-frequency band which extends to $\sim$170 cm^{-1}. This is well beyond any theoretical or experimental phonon dispersion curves, which suggest $\omega_{\max}<150$ cm^{-1}. One aspect of ρ_T which cannot be accounted for in either ρ_N or SORS is the sharp peak at $\sim$147 cm^{-1}. This suggests that some modification is needed in the model for the highest-frequency phonons.

While enhanced scattering in Te from combination OP$^{(1)}$ and OP$^{(2)}$ bands might imply similar nonovertone scattering from the 2OP$^{(1)}$ and 2OP$^{(2)}$ terms, the agreement between experiment and a more detailed theory suggests that overtone scattering is likely still predominant for the form of these bands.

The SORS of polycrystalline t-Se, shown in Fig. 3(a), was obtained at 300 K. The spectrum, whose frequency scale has been halved, is similar to that previously obtained by Mooradian and Wright[4] (MW) at low temperatures. Previously, the SORS of t-Se has been interpreted in terms of $2k=0$ processes by Lucovsky *et al.*[3] and as a combined density of states by Geick and Schroder.[19] However, a comparison with recent inelastic neutron scattering measurements of Gompf[1] indicates that all the major peaks in the second-order Raman spectrum of t-Se

correspond to features in the one-phonon density of states. We consequently deduce that the main features in the former spectrum are due predominantly to overtone scattering. This is demonstrated in Fig. 3, which shows a comparison of the second-order Raman spectrum with the phonon density of states obtained from neutron scattering and a theoretical density of states ρ_T of Etchepare *et al.*[18] Etchepare *et al.* employed a valence force model similar to that used for *t*-Te.

While a portion of the low-frequency band is obscured by the very intense first-order peaks centered at 143 and 235 cm^{-1} (shown at half their frequency), the main low-frequency density-of-states features may still be observed at 39, 53, 92, 105, and 138 cm^{-1}. All but the 105-cm^{-1} feature correspond, within 6 cm^{-1}, to features in ρ_N at 45, 55, 92, and 134 cm^{-1}. The shoulder at 105 cm^{-1}, which may be the result of combination processes, is not shown in Fig. 3 as it is on the rising slope of the first-order peak at $\sim$233 cm^{-1}. A feature in the SORS corresponding to the shoulder in ρ_N at 122 cm^{-1} may also be obscured by this first-order peak.

In comparing ρ_T to ρ_N and the SORS for this low-frequency band, it is observed that ρ_T appears to correctly exhibit many of the qualitative features of the density of states. The actual frequency of these features in ρ_T differ, though, from those in the SORS and ρ_N, by $\sim$15 cm^{-1}. In addition, well-defined gaps predicted by ρ_T are not seen in either the SORS or ρ_N. Etchepare *et al.*[18] have assigned the features at $\sim$40 and $\sim$55 cm^{-1} to chain torsional motions, while the feature at $\sim$92 cm^{-1} is assigned to librations and those at $\sim$122 and $\sim$135 cm^{-1} to bond-bending modes.

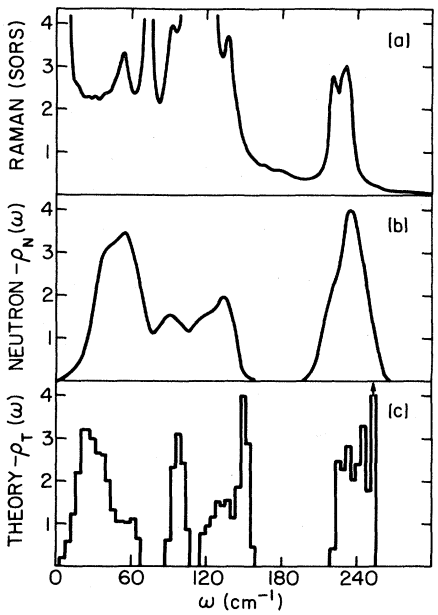

FIG. 3. Comparison of (a) the Raman spectra of *t*-Se with (b) the neutron scattering–determined density of states of Ref. 1 and (c) the theoretical density of states of Ref. 18. The frequency scale of (a) has been halved for comparison.

Between $\sim$142 and $\sim$200 cm^{-1}, Fig. 3(a) exhibits features in the SORS which are not observed in ρ_N or ρ_T. These features lie in the region where ρ_T predicts and ρ_N shows a gap in the density of states. This structure thus originates from $OP^{(1)}+OP^{(2)}$ combination processes. It is useful to note that the intensities of these features are weak as compared to the overtone attributed processes. This is the case in most elemental systems except for *t*-Te. Between $\sim$25–35 cm^{-1}, the spectrum of Fig. 3(a) is relatively constant in intensity while the stray-light background contribution for the third monochromator system is estimated to be small. This suggests low-frequency second-order scattering which is unresolved. Sharp features observed below 33 cm^{-1} which are also present may imply a contribution from difference processes at low frequencies in *t*-Se.

In the high-frequency band of *t*-Se, the peaks in the SORS at halved frequencies of 221 and 231 cm^{-1} correspond reasonably well with a shoulder at $\sim$220 cm^{-1} and a peak at 234 cm^{-1} in ρ_N. However, a large density of states is shown in ρ_N on the high-frequency side. This is not seen in the SORS, which exhibits an extended low-intensity tail. The relatively low resolution of neutron scattering should yield some broadening of the density of states, although this might be expected to be relatively symmetric and therefore cannot alone account for these high-frequency states. The second-order infrared-absorption spectrum of *t*-Se (Ref. 20) exhibits two high-frequency peaks at $\sim$229 and $\sim$239 cm^{-1}. While these peaks do not occur near the peaks of ρ_N or the SORS, they do imply the presence of high-frequency states. This suggests that matrix-element effects may perhaps be suppressing some higher-frequency states in the SORS. In contrast, a smoothing of ρ_T would create a double-peaked structure which is, however, too high in frequency compared to ρ_N and the SORS. The sharp peak shown at 252 cm^{-1} in the theoretical histogram of Fig. 3(c) cannot be accounted for by either ρ_N or the SORS. Both the shape and location of this band in ρ_T more nearly resemble the Raman spectra of amorphous Se (Refs. 21 and 22) than *t*-Se. This suggests that the model of Etchepare *et al.* may underestimate the strengths of interchain bonding which is weaker in *a*-Se than it is in *t*-Se and has the effect of shifting the high-frequency band to increasing frequencies.

It is instructive to compare the SORS of t-Te in Fig. 2 with t-Se in Fig. 3. Whereas the t-Te spectrum exhibits broad features, the t-Se spectrum contains relatively sharp peaks. Sharper features in the density of states are indicative of less dispersion in the phonon dispersion curves. This can be attributed to t-Se having greater covalent character than t-Te due to weaker interchain interactions. The higher optic region of t-Se shows a double-peaked structure with the most intense peak on the high-frequency side of this band. In the same region of the t-Te spectrum the two features appear as a peak and a shoulder with the peak on the low-frequency side of the band. It has been shown that an effect of stronger interchain interaction in t-Te is to decrease the frequency of the first-order symmetric A_1 breathing model relative to an E stretching mode.[23] The SORS of t-Te suggests that the related zone-boundary high-frequency phonon states are lowered in frequency to the point where the two-peaked structure of t-Se no longer exists and a larger number of states reside on the low-frequency side of the band.

B. Raman spectra of m-Se and o-S

First-order Raman studies have previously been performed on both m-Se (Ref. 4) and o-S.[24] Theory predicts 93 modes for o-S, of which 48 are Raman active. Of these, 29 modes have been observed by means of high-resolution work done by Anderson and Loh.[25] Eleven modes, some split from crystal-field effects, have been identified as vibrations of the S_8 molecule. The first-order Raman spectrum of m-Se has been obtained by Mooradian and Wright.[4] Assignments of Se_8 vibrational modes were made by a comparison to the o-S spectra using a frequency scaling factor of ~ 1.9. First-order spectra obtained from both o-S and m-Se were very similar to these earlier studies. For m-Se, our spectra above 35 cm^{-1} was identical to those of MW. An exception was the observation of three additional frequency peaks at 16, 26, and 32 cm^{-1} due to improved stray-light rejection.

The SORS of m-Se and o-S, which have been presented earlier,[26,27] are shown in Figs. 4(a) and 4(b), respectively. The dashed lines indicate the tails of the first-order peaks which are ~ 100 times more intense than the second-order peaks in m-Se and ~ 400 times more intense in o-S. The arrows indicate twice the frequency of the $k=0$ Raman modes at room temperature and are labeled with their molecular-mode assignments. Both spectra can be separated into three distinct regions. The lowest-frequency region is bounded by a gap in the first-order modes between 128 and 240 cm^{-1} in m-Se and

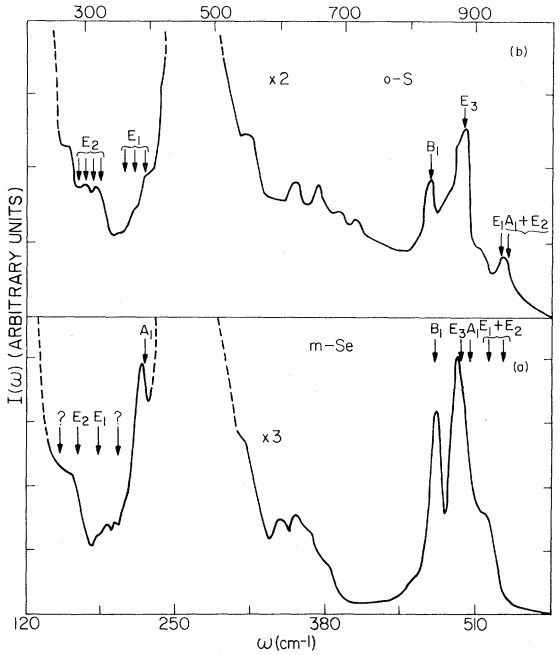

FIG. 4. Comparison of (a) the second-order Raman spectra of m-Se with (b) o-S. The vertical arrows and letters correspond to the doubled frequencies of the first-order $k=0$ modes.

between 255 and 420 cm^{-1} in o-S. A second region starts at the tail of the first-order mode and extends to a relative minima at 420 cm^{-1} in m-Se and 760 cm^{-1} in o-S. The third region is a high-frequency band containing a three-peaked structure.

The gap region in the SORS of m-Se consists of three spectral features. A shoulder at ~ 160 cm^{-1} lies near twice the frequency of an E_2 mode. A sharp peak at 220 cm^{-1} corresponds closely to twice the A_1 mode at 112 cm^{-1}. The location of this latter feature suggests that its origin is due to overtones from the phonon branch corresponding to the 112-cm^{-1}, $k=0$ mode. The sharpness of the SORS peak suggests that there is little dispersion in this band. Similarly, the shoulder at ~ 160 cm^{-1} is expected to originate from overtones of the 83-cm^{-1}, $E_1, k=0$ phonon branch. The gap region in o-S exhibits somewhat similar structure to the corresponding spectral region in m-Se. Two features at ~ 300 and ~ 320 cm^{-1} correspond to twice the frequency of the fourfold-split E_2 mode. This parallels the shoulder at 160 cm^{-1} in m-Se. Three shoulders on the rising tail of the first-order peak at 142 cm^{-1} correspond to twice the frequency of the threefold-split E_1 mode. This again parallels features in the m-Se SORS for the E_1 mode. A feature that would parallel the sharp second-order A_1 peak in m-Se could not be detected since in o-S the corresponding

A_1 mode is at 219 cm^{-1} and the first-order peak at 437 cm^{-1} obscures any second-order features.

The second region between 300–420 cm^{-1} in *m*-Se and 500–760 cm^{-1} in *o*-S corresponds to a frequency range which is well separated from twice the frequency of any $k=0$ modes and where there is, therefore, expected a gap in the density of states. Both *m*-Se and *o*-S again show very similar features in this region which can be interpreted as originating from combination processes between high-frequency and low-frequency optic phonons.

The third region of the second-order scattering consists only of overtones and combinations between the higher optic modes. In *m*-Se the narrow peaks at 478 and 496 cm^{-1} are both very near to twice the frequency of $k=0$ modes observed in the first-order spectrum. Their location therefore strongly suggests that these peaks are due primarily to overtones. Their narrowness suggests little dispersion in the phonon branches, although a relatively weak low-frequency shoulder at 460 cm^{-1} suggests that this branch has some dispersion to lower frequencies. On the high-frequency tail of the peak at 469 cm^{-1} there exists a shoulder at ~ 520 cm^{-1}. The location of the three $k=0$ Raman modes shown suggest that this feature is also due to overtones.

The corresponding band for *o*-S in Fig. 4(b) also contains two prominent peaks at 822 and 876 cm^{-1}. The high-frequency peak at 937 cm^{-1}, which appeared as a shoulder in *m*-Se, is now resolved in *o*-S. The distinct nature of this peak is attributed to reduced dispersion relative to *m*-Se. Shoulders at 900 and 866 cm^{-1} could be an indication of combination processes between the modes, although they might also be due to some dispersion in the phonon branches. As in *m*-Se, the major high-frequency features occur very close to twice the values of the $k=0$ modes. No Raman- or infrared-active $k=0$ modes occur near one-half the second-order peak at 822 cm^{-1}. However, a normal-mode analysis by Scott *et al.*[28] predicts a B_1 mode at 412 cm^{-1} which is strictly inactive in an isolated molecule. Scott *et al.* have produced indirect evidence of this mode at 411 cm^{-1} through a combination band in the infrared spectrum of *o*-S. Anderson and Loh observed a peak in their low-temperature, high-resolution Raman spectra of *o*-S at 417 cm^{-1}. They assigned this weak peak to the B_1 mode which may be seen as a weak feature in *o*-S due to crystal-field effects. At room temperature, the frequency of this peak may be somewhat lower. This mode is thus very near half the frequency of the peak in the SORS, again suggesting overtone scattering.

These results and the similarity of the high-frequency bands of the SORS of *m*-Se and *o*-S suggest a revised mode assignment for the first-order peaks in *m*-Se. The first peak in the high-frequency band of *o*-S is assigned to overtones from a B_1 mode which is weakly observed in the Raman spectra. The first peak of *m*-Se in this same region would be assigned to overtones from an E_3 mode if a previous assignment is correct.[3] The second peak and shoulder would also have different assignments in *m*-Se than in *o*-S. If, however, we assign the lowest high-frequency first-order mode at 237 cm^{-1} of *m*-Se to B_1 and then shift each of the assignments upward by one peak, then the symmetry assignments of the second-order peaks of *m*-Se and *o*-S are the same. This would be totally consistent since (1) the first-order peak at 237 cm^{-1} is very weak as would be expected of a B_1 mode, (2) the A_1 mode now has a very large relative intensity compared to the other peaks as is expected, and (3) all of the high-frequency first-order modes now have an assignment in terms of an eight-membered ring vibration. These new assignments are indicated in Table I and are employed in Fig. 4.

C. Comparison of the high-frequency bands and electronic states

A comparison of the high-frequency SORS bands after background subtraction of *t*-Te, *t*-Se, *m*-Se, and *o*-S is shown in Fig. 5. A scaling factor of 1.64 is used to align the 268-cm^{-1} peak of the *t*-Te spectrum[29] to the 441-cm^{-1} peak of the *t*-Se spectrum. If the force constants for the vibrations between atoms were equal for *t*-Te and *t*-Se, then the frequencies would scale with the square root of the mass ratio, i.e., $(m_{Te}/m_{Se})^{1/2}=1.27$. In contrast, the larger empirical factor of 1.64 indicates that *t*-Te has a lower average effective force constant than *t*-Se. The scaling factor used to align the most intense peaks of *o*-S and *m*-Se is 1.77. Again, this is a larger value than the square root of the mass ratio, $(m_{Se}/m_S)^{1/2}=1.58$. This indicates a trend of weaker intraunit bonding in *t*-Te than in *t*-Se and in *m*-Se relative to *o*-S. This also demonstrates that intraunit covalent bonding increases as interunit bonding de-

TABLE I. High-frequency first-order modes of *m*-Se at $k=0$.

Frequency (cm^{-1})	Previous assignment[a]	New assignment
237	E_3	B_1
248	A_1	E_3
252	E_2	A_1
260	E_1	E_1 or E_2
266		E_1 or E_2

[a]Reference 3.

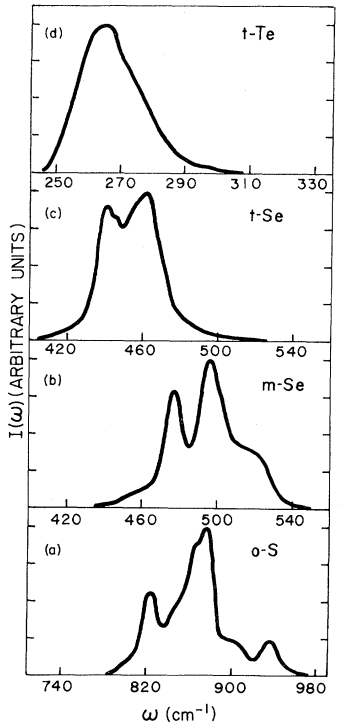

FIG. 5. Comparison of the high-frequency optic bands of (a) *o*-S, (b) *m*-Se, (c) *t*-Se, and (d) *t*-Te.

creases in these group-VI elements.

Dultz *et al.*[30] and Meek[31] have suggested that a high-frequency two-peaked structure in the phonon density of states is characteristic of isolated chains. Figure 5 indicates a progression from a single peak in the density of states of *t*-Te to a multipeak structure in *o*-S. The double-peaked structure of *t*-Se is consistent with theory, while the single-peaked structure in *t*-Te is a likely consequence of significant interchain interactions which result in enhanced dispersions and band overlap. The high-frequency, scaled spectra of *o*-S and *m*-Se are similar in form, indicating essentially three distinct bands for weakly coupled rings. The intensity of the spectra above ~ 510 cm^{-1} in *m*-Se and ~ 890 cm^{-1} in *o*-S in Fig. 5 are, however, reduced relative to a dispersionless model of the phonons. In particular, such a molecular model would predict five bands.[28] Based on the first-order Raman spectral lines in Fig. 4 the highest three bands would be nearly degenerate. In contrast, the high-frequency band intensities in Fig. 5 are of lower intensity. This may be a consequence of either a diminished matrix-element variation at high-frequency, finite phonon dispersion, which shifts states to lower frequency from their $k=0$ values, or a combination contribution near the band center. Phonon dispersion effects might imply, given the excellent correspondence in Fig. 4 between $k=0$ and SORS peaks, bands of both narrow and wider dispersion. Both the electronic properties of *o*-S as well as the Raman spectra of liquid (*l*-) S suggest some overlap of molecularlike bands. Time-of-flight neutron scattering measurements in polycrystalline *o*-S would thus be useful in separating dispersion effects from matrix-element effects or combinations that may influence the relative second-order peak intensities.

In *m*-Se the band center is shifted by ~ 34 cm^{-1} to higher frequency relative to *t*-Se. This shift, which corresponds to 17 cm^{-1} in the phonon density of states, is attributed to the influence of stronger interunit interactions in *t*-Se. In general, the spectra of Fig. 5 indicate that with decreasing atomic number the phonon bands become sharper, suggesting increased covalent interactions and greater molecular behavior in the lighter elements, as is expected. The trend of decreasing phonon dispersion parallels that observed in the photoemission studies of the valence-band density of states, where, e.g., additional features are observed in both the bonding *p* and *s* bands in *o*-S relative to *m*-Se. This is most clearly observed for the *s* band of *o*-S where five peaks have been assigned to the two singly degenerate and three doubly degenerate ring modes of an eight-membered ring.[32] In *m*-Se the presence of three rather than five peaks has been suggested to arise from *d*-state hybridization within a ring. The absence, however, of cross-section—enhanced *d*-electron scattering suggests, alternatively, the possibility that weak interring interactions may also modify the valence-band dispersion of *m*-Se relative to *o*-S.[33] Since the first- and second-order Raman spectra suggest that *m*-Se may have phonon branches that have some dispersion, this system may not be quite as molecular in character as *o*-S. As the interring to intraring distance ratio is ~ 1.70 in *o*-S vs 1.62 in *m*-Se, it is possible that more prototypical van der Waal—type bonding occurs in the former.

D. Comparison of crystalline and noncrystalline phases

In noncrystalline amorphous and liquid systems the scattering intensity for first-order processes yields a coupling-parameter—weighted phonon density of states that is analogous to that obtained for second-order crystalline systems for dominant overtone scattering. Previous comparisons of the changes in the phonon spectra of *t*-Te and amorphous (*a*-) Te have, however, contrasted the discrete $k=0$ crystalline first-order scattering with the continuum *a*-Te spectrum.[13] The present results allow a more valid direct comparison of the respective spec-

trally weighted densities of states. Under the reasonable assumption of smoothly varying coupling parameters for the SORS in *t*-Te and first-order scattering in *a*-Te, an estimate of changes in the vibrational spectra with disorder may be obtained. In *t*-Te the high-frequency optic peak from Fig. 5(d) occurs at 134 cm^{-1} with a full width at half maximum of ~ 11 cm^{-1}. The corresponding peak in *a*-Te occurs at 150 cm^{-1} with a width of ~ 30 cm^{-1}. The factor-of-3 increase in width in *a*-Te is attributed to considerable structural disorder with primary contributions from intrachain as well as interchain disorder. The shift of the peak to higher frequencies by 12% in *a*-Te has been qualitatively noted earlier[34] and interpreted as a consequence of decreasing interchain and corresponding increasing intrachain interactions in the amorphous state. For the lower optic modes, the neutron and Raman results of Fig. 2 imply two peaks in *t*-Te between 75 and 95 cm^{-1}, while the amorphous spectra indicate a single peak at ~ 90 cm^{-1}.

The first-order Raman spectra of bulk[21,22] and thin-film[35–38] *a*-Se exhibit a high-frequency peak at 250 cm^{-1} and a shoulder at ~ 239 cm^{-1}. Recent second-order Raman scattering measurements in *a*-Se suggest a coupling-parameter enhancement of the former polarized peak in the first-order spectra.[39] Thus the density of states of the high-frequency opticlike band of *a*-Se exhibits two features of comparable intensity, which are shifted to higher frequency relative to *t*-Se. This shift is attributed to reduced interchain coupling in *a*-Se that is analogous to the shift observed in *m*-Se due to reduced interunit interactions. In contrast to *m*-Se, however, the spectra of *a*-Se have suggested a small number of rings.[21] The recent results, which indicated a three-peak structure for the phonon spectrum of *m*-Se relative to two features in *a*-Se, are consistent with this model. In the Se system the shift of the high-frequency density of states of *a*-Se relative to *t*-Se is $\sim \frac{3}{4}$ that between *a*-Te and *t*-Te. This is consistent with decreased interchain coupling in *a*-Se or increased interchain coupling in *t*-Te.

The high-frequency first-order *VH* Raman spectra[24] of liquid (*l*-) S near T_{melt} exhibit three peaks of comparable integrated intensities at 430, 441, and 474 cm^{-1}. These correspond to the three SORS peaks observed in *o*-S in Fig. 5(a) at twice 411, 438, and 469 cm^{-1}. Lower-frequency peaks in *l*-S at ~ 151 cm^{-1} and 218 cm^{-1} also correspond to similar peaks in *o*-S at twice these frequencies, while the peak associated with the ~ 240-cm^{-1} line in *l*-S is obscured in *o*-S by a first-order peak. These results are thus consistent with predominant overtone scattering in *o*-S and *m*-Se. It is useful to note that *a*-S prepared under conditions that prevent S_8 in the vapor phase[24] or which extract most S_8 molecules to form predominantly fibrous S composed of chains,[30] indicates two rather than three high-frequency phonon density-of-states peaks similar to that observed in *t*-Se and *a*-Se. These results indicate that the three high-frequency peak structures observed in *m*-Se, *o*-S, and *l*-S are attributable to the presence of rings, whereas crystalline *t*-Se and noncrystalline chain structures of Se and S exhibit two peaks. These results are consistent with the interpretation of the first- and second-order Raman spectra of *a*-Se in terms of predominant chain configurations with a small number of rings.[21]

IV. SUMMARY AND CONCLUSIONS

Second-order Raman scattering in the group-VI elemental semiconductors has been interpreted in terms of overtone and combination processes. The former determine the features of the SORS processes in the spectral regions corresponding to twice the $OP^{(1)}$ and $OP^{(2)}$ contributions. As in other elemental semiconductors and semimetals, overtones also exhibit considerably larger scattering than $OP^{(1)}+OP^{(2)}$ combinations, though the latter is enhanced in *t*-Te. A comparison of the form of the phonon density of states deduced under the reasonable assumption of weak coupling-parameter variations yields good agreement with a theoretical model of Etchepare *et al.* for *t*-Te and reasonable agreement for *t*-Se though both models appear to have an excess of states near the maximum phonon frequency. In the sequence *t*-Te, *t*-Se, *m*-Se, and *o*-S corresponding to the transition from chain to ring structures, the phonon spectra for the $OP^{(2)}$ band exhibit decreased dispersion and additional features which are consistent with increasing molecular and decreasing metallic or delocalized bonding. The trend is similar to that observed in x-ray photoemission measurements for *s*-band states, though some dispersion in *m*-Se phonon branches suggests that intermolecular coupling is stronger in *m*-Se than *o*-S.

A comparison with the phonon spectra of the crystalline, amorphous, and liquid counterparts also indicates the increasing importance of covalent nearest-neighbor interactions in the noncrystalline phases. The results suggest additional features in the phonon spectrum for the highest optic band for ring structures relative to chains in both crystalline and noncrystalline phases.

ACKNOWLEDGMENTS

We wish to thank Professor K. Vedam for the *t*-Se sample and Dr. R. Zallen for the *m*-Se specimen. This research was supported in part by National Science Foundation Grant No. DMR-81-09033.

*Present address.

[1]F. Gompf, in *The Physics of Selenium and Tellurium,* edited by E. Gerlach and P. Grosse (Springer, Berlin, 1979), p. 64.

[2]J. Stuke, in *Selenium,* edited by R. A. Zingaro and W. C. Cooper (Van Nostrand Rheinhold, New York, 1974), p. 174.

[3]G. Lucovsky, A. Mooradian, W. Taylor, G. B. Wright, and R. C. Keezer, Solid State Commun. 5, 113 (1967).

[4]A. Mooradian and G. B. Wright, in *The Physics of Selenium and Tellurium,* edited by W. C. Cooper (Pergamon, Oxford, 1969), p. 269.

[5]B. M. Powell and P. Martel, J. Phys. Chem. Solids 36, 1287 (1975).

[6]W. C. Hamilton, B. Lassier, and H. I. Kay, J. Phys. Chem. Solids 35, 1089 (1974).

[7]W. D. Teuchert, R. Geick, G. Landwehr, H. Wendel, and W. Weber, J. Phys. C 8, 3725 (1975).

[8]P. A. Temple and C. E. Hathaway, Phys. Rev. B 7, 3685 (1973).

[9]B. A. Weinstein and M. Cardona, Phys. Rev. B 7, 2545 (1973).

[10]J. S. Lannin, J. M. Calleja, and M. Cardona, Phys. Rev. B 12, 585 (1975).

[11]J. S. Lannin and B. V. Shanabrook, in *Physics of Semiconductors, 1978,* edited by B. L. Wilson (IOP, London, 1979), p. 643.

[12]B. V. Shanabrook and J. S. Lannin, Solid State Commun. 38, 49 (1981).

[13]M. H. Brodsky, R. J. Gambino, J. E. Smith, Jr., and Y. Yacoby, Phys. Status Solidi B 52, 509 (1972).

[14]B. A. Kotov, N. M. Okuneva, and A. L. Shakn-Budagov, Fiz. Tverd. Tela 9, 2553 (1967) [Sov. Phys.—Solid State, 9, 2011 (1968)].

[15]A. Pine and G. Dresselhaus, Phys. Rev. B 4, 356 (1971).

[16]B. M. Powell and P. Martel, J. Phys. Chem. Solids 36, 1287 (1975).

[17]B. Orel, R. Turbino, and G. Zerbi, Mol. Phys. 30, 37 (1975).

[18]J. Etchepare, P. Kaplan, and M. Merian, in *Proceedings of the International Conference on Lattice Dynamics,* edited by M. Balkanski (Flammarion, Paris, 1977), p. 60.

[19]G. Geik and U. Schröder, in *The Physics of Selenium and Tellurium,* edited by W. C. Cooper (Pergamon, Oxford, 1969), p. 277.

[20]R. S. Caldwell and H. Y. Fan, Phys. Rev. 114, 664 (1959).

[21]P. J. Carroll and J. S. Lannin, J. Non-Cryst. Solids 36, 1277 (1980).

[22]M. Gorman and S. A. Solin, Solid State Commun. 18, 1401 (1976).

[23]G. Lucovsky, Phys. Status Solidi B 49, 633 (1972).

[24]A. T. Ward, J. Phys. Chem. 72, 4133 (1968).

[25]A. Anderson and Y. T. Loh, Can. J. Chem. 47, 879 (1969).

[26]P. J. Carroll and J. S. Lannin, J. Phys. Soc. Jpn., Suppl. A, 49, 669 (1980).

[27]P. J. Carroll and J. S. Lannin, J. Phys. (Paris) Colloq. 42, C6-643 (1981).

[28]D. W. Scott, J. P. McCullough, and F. H. Kruse, J. Mol. Spectrosc. 13, 313 (1964).

[29]The scale on the *t*-Te figure in Ref. 27 is low by 10 cm^{-1}.

[30]W. Dultz, H. D. Hochheimer, and W. Müller-Lierheim, in *Proceedings of the Fifth International Conference on Amorphous and Liquid Semiconductors,* edited by J. Stuke and W. Brenig (Taylor and Francis, London, 1974), p. 1281.

[31]P. E. Meek, Philos. Mag. 34, 767 (1976).

[32]W. R. Salaneck, C. B. Duke, A. Paton, C. Griffiths, and R. C. Keezer, Phys. Rev. B 15, 1100 (1977).

[33]N. J. Shevchik, J. Phys. C 8, 3767 (1975).

[34]P. J. Carroll and J. S. Lannin, in *Proceedings of the Seventh International Conference on Raman Spectroscopy,* edited by W. F. Murphy (North-Holland, New York, 1980), p. 66.

[35]J. E. Smith, Jr., M. H. Brodsky, and R. J. Gambino, Bull. Am. Phys. Soc. II 17, 336 (1972).

[36]C. C. Tsai and R. J. Nemanich, J. Non-Cryst. Solids 36, 1203 (1980).

[37]N. Ohta, W. Scheuermann, and K. Nakamoto, Solid State Commun. 27, 1325 (1978).

[38]P. J. Carroll and J. S. Lannin, Solid State Commun. 40, 81 (1981).

[39]J. S. Lannin and P. J. Carroll, Philos. Mag. 45, 155 (1982).